An electronegativity model for the fundamental infrared intensities of the halomethanes

I.S. Scarminio[a], B. de Barros Neto[b], A.E. de Oliveira[c], R.L.A. Haiduke[c], R.E. Bruns[c],*

[a]*Departamento de Química, Universidade Estadual de Londrina, CP 6001, 86051-970 Londrina, PR, Brazil*
[b]*Departamento de Química Fundamental, Universidade Federal de Pernambuco 50740-250 Recife, PE, Brazil*
[c]*Instituto de Química, Universidade Estadual de Campinas, CP 6154, 13083-970 Campinas, SP, Brazil*

Abstract

A principal component analysis of halomethane polar tensor invariant data shows that four of the five invariant quantities, the atomic mean dipole moment derivative, $\bar{p}_\alpha$, effective charge, χ_α, determinant, D_α, and minor sum, C_α, are linearly related to changes in substituent electronegativities. The atomic anisotropy, β_α^2, has a completely different behavior. Based on a linear regression equation involving χ_α and the substituent electronegativity change and the G intensity sum rule an electronegativity model is proposed for estimating the halomethane intensity sums. A single equation involving substituent electronegativities and atomic masses can be used to estimate intensity sums that are in good agreement with experimental values. This expression permits an understanding of intensity sum trends for the halomethanes in terms of the electronegativities and atomic masses of the substituent atoms. © 2001 Elsevier Science Ltd All rights reserved.

Keywords: Infrared intensities; Electronegativity models; Halomethanes; Principal components; Dipole moment derivatives

1. Introduction

Ten years ago our research group reported the results of an exploratory analysis [1] of polar tensor data for about 50 molecules for which complete gas phase infrared fundamental intensity data had been reported in the literature. This study employed the chemometric multivariate analysis and revealed a systematic behavior in the carbon atomic polar tensor data that had not been recognized before. Previously focus had been given to polar tensors of terminal atoms and the possibilities of their transference to other molecules with the aim of predicting infrared intensities. The exploratory analysis led to the development of electronegativity models for the carbon

atom polar tensor parameters [2,3]. Polar tensor parameters for terminal atoms were also found to be dependent on their own electronegativities and a separate model was developed for them.

This work is limited to a chemometric exploratory analysis of polar tensor data for the halomethanes with the aim of further developing electronegativity models for estimating infrared intensities. The halomethanes were chosen for two reasons. Firstly, considerable effort has been made in recent years to measure infrared intensities of some halomethanes with greater accuracy, particularly the fluorochloromethanes in studies considering the possibility of infrared remote sensing of their concentrations in the atmosphere. Results of more recent measurements, not used in our previous exploratory analysis, have been included here. Secondly, halogen atom

* Corresponding author.

substitution of hydrogen in methane results in changes of carbon polar tensor values significantly larger than variations owing to measurement errors in gas phase intensity determinations. Advantage of this favorable situation is taken to study how carbon polar tensors in the halomethanes are related to basic chemical valency parameters, especially electronegativity.

The chemometric analysis leads to the proposal of a single electronegativity regression model including effects of both the central carbon and terminal halogen and hydrogen atoms that is useful for estimating infrared fundamental intensity sums. As in our previous work five atomic polar tensor invariant quantities, the atomic mean dipole moment derivative, $\bar{p}_\alpha$, atomic anisotropy, β_α^2, squared atomic effective charge, χ_α^2, determinant, D_α, and sum of the minors of the diagonal elements, C_α, with $\alpha = $ C, H, F, Cl, Br and I are investigated. In the exploratory analysis using principal components the data set is preprocessed so that all invariant quantities have identical units, here electrons. For this reason square roots of χ_α^2, β_α^2 and C_α and the cubic root of D_α were taken to be analyzed along with the mean dipole moment derivative values.

At this point it should be mentioned why model development of the type performed here is worthwhile even though infrared intensities can be calculated with acceptable accuracy by quantum chemical methods for many chemical applications. Modeling techniques permit an increased understanding of the data being examined, and how this data varies with variations in basic chemical valency quantities. Furthermore electronegativity models for infrared intensities have already shown their usefulness since they have been related to electronegativity models for core electron ionization energies. This permitted the development of a potential model showing how core ionization energies vary with a mean dipole moment derivatives providing greater understanding of both experimental quantities, one measured in the X-ray region of the electromagnetic spectrum and the other in the infrared [4].

2. Calculations

Within the harmonic oscillator–linear dipole moment approximations the measured fundamental infrared intensity, A_i, is proportional to the square of the dipole moment derivative with respect to its associated normal coordinate, Q_i,

$$A_i = \frac{N_A \pi}{3c^2} \left(\frac{\partial \vec{p}}{\partial Q_i} \right)^2, \tag{1}$$

N_A and c being Avogadro's number and the velocity of light, respectively [5]. The dipole moment derivatives can be transformed to atomic Cartesian coordinates using the expression [6,7]

$$\mathbf{P}_x = \mathbf{P}_Q \mathbf{L}^{-1} \mathbf{U} \mathbf{B} + \mathbf{P}_\rho \boldsymbol{\beta}, \tag{2}$$

where $\mathbf{P}_Q$ is a $3 \times 3N - 6$ matrix of the dipole moment derivatives, $\partial \vec{p} / \partial Q_i$, obtained from the measured infrared intensities and $\mathbf{L}^{-1}$, $\mathbf{U}$ and $\mathbf{B}$ are the well-known transformation matrices commonly used in normal coordinate analysis [8]. The $\mathbf{P}_\rho \boldsymbol{\beta}$ product provides the rotational contributions to the polar tensor elements. As such the polar tensor elements contained in $\mathbf{P}_x$ are obtained using the molecular geometry (the $\mathbf{B}$ and $\boldsymbol{\beta}$ matrices), symmetry (the $\mathbf{U}$ matrix), vibrational frequencies and atomic masses (the normal coordinate $\mathbf{L}^{-1}$ matrix) and permanent dipole moment values, as well as the experimentally measured intensities ($\mathbf{P}_Q$, dipole moment derivative matrix).

The molecular polar tensor, $\mathbf{P}_x$, is a juxtaposition of the atomic polar tensors (APTs)

$$\mathbf{P}_x = \{\mathbf{P}_x^{(1)} \mathbf{P}_x^{(2)} ... \mathbf{P}_x^{(N)}\} \tag{3}$$

with N being the number of atoms in the molecule. Each APT contains the derivatives of the molecular dipole moment with respect to the atomic Cartesian coordinates,

$$\mathbf{P}_x^{(\alpha)} = \begin{pmatrix} \partial p_x/\partial x_\alpha & \partial p_x/\partial y_\alpha & \partial p_x/\partial z_\alpha \\ \partial p_y/\partial x_\alpha & \partial p_y/\partial y_\alpha & \partial p_y/\partial z_\alpha \\ \partial p_z/\partial x_\alpha & \partial p_z/\partial y_\alpha & \partial p_z/\partial z_\alpha \end{pmatrix}$$

$$= \begin{pmatrix} p_{xx} & p_{xy} & p_{xz} \\ p_{yx} & p_{yy} & p_{yz} \\ p_{zx} & p_{zy} & p_{zz} \end{pmatrix}. \tag{4}$$

The mean dipole moment derivative of atom α, $\bar{p}_\alpha$, is simply 1/3 the trace of this matrix [9]

$$\bar{p}_\alpha = 1/3(\partial p_x/\partial x_\alpha + \partial p_y/\partial y_\alpha + \partial p_z/\partial z_\alpha). \tag{5}$$

Table 1
Exp. polar tensor invariant quantities for the halomethanes, units of electrons, (e)

| Molecule	Atom	$\bar{p}_\alpha$	β_α	χ_α	$D_\alpha^{1/3}$	$|C_\alpha|^{1/2}$
CH$_4$ [10]	C	0.016	0.000	0.016	0.016	0.028
	H	−0.004	0.114	0.054	0.026	0.066
CH$_3$F [9,11,12]	C	0.541	0.579	0.606	0.482	0.875
	H	−0.017	0.200	0.096	−0.056	0.106
	F	−0.490	0.665	0.581	−0.406	0.756
CH$_2$F$_2$ [13,14]	C	1.105	0.645	1.059	0.971	1.718
	H	−0.018	0.162	0.079	−0.041	0.073
	F	−0.488	0.639	0.574	−0.415	0.766
CHF$_3$ [15,16]	C	1.523	0.567	1.546	1.497	2.617
	H	0.042	0.023	0.043	0.040	0.071
	F	−0.507	0.647	0.591	−0.435	0.800
CF$_4$ [17]	C	2.051	0.000	2.051	2.051	3.552
	F	−0.512	0.411	0.547	−0.472	0.855
CH$_3$Cl [18,19]	C	0.277	0.496	0.363	0.197	0.386
	H	−0.002	0.156	0.074	0.000	0.088
	Cl	−0.271	0.281	0.301	−0.243	0.440
CH$_2$Cl$_2$ [20]	C	0.531	0.887	0.676	0.378	0.764
	H	−0.008	0.108	0.052	0.048	0.060
	Cl	−0.258	0.453	0.335	−0.195	0.374
CHCl$_3$ [21,22]	C	0.826	0.951	0.940	0.631	1.321
	H	−0.022	0.089	0.048	0.046	0.034
	Cl	−0.267	0.552	0.373	−0.158	0.346
CCl$_4$ [23]	C	1.043	0.000	1.043	1.043	1.807
	Cl	−0.261	0.398	0.322	−0.158	0.389
CF$_3$Cl [24]	C	2.033	0.680	2.058	2.009	3.499
	F	−0.629	0.631	0.695	−0.571	1.047
	Cl	−0.148	0.299	0.204	−0.93	0.189
CF$_2$Cl$_2$ [24]	C	1.636	0.433	1.649	1.623	2.823
	F	−0.585	0.653	0.661	−0.516	0.941
	Cl	−0.233	0.562	0.353	−0.114	0.251
CFCl$_3$ [24]	C	1.352	0.165	1.354	1.350	2.340
	F	−0.514	0.687	0.608	−0.429	0.797
	Cl	−0.279	0.688	0.428	−0.137	0.324
CH$_3$Br [18,25]	C	0.210	0.469	0.305	0.115	0.243
	H	−0.001	0.163	0.077	−0.030	0.094
	Br	−0.204	0.180	0.221	−0.189	0.338
CH$_3$I [18]	C	0.134	0.341	0.209	0.052	0.122
	H	−0.049	0.122	0.075	−0.582	0.095
	I	−0.114	0.003	0.114	−0.114	0.197
CF$_3$Br [26]	C	1.722	0.794	1.762	1.684	2.947
	F	−0.537	0.817	0.661	−0.401	0.803
	Br	−0.112	0.364	0.205	−0.031	0.079
CF$_3$I [26]	C	1.765	1.082	1.837	1.699	2.992
	F	−0.576	0.923	0.722	−0.414	0.848
	I	−0.036	0.307	0.149	−0.102	0.166
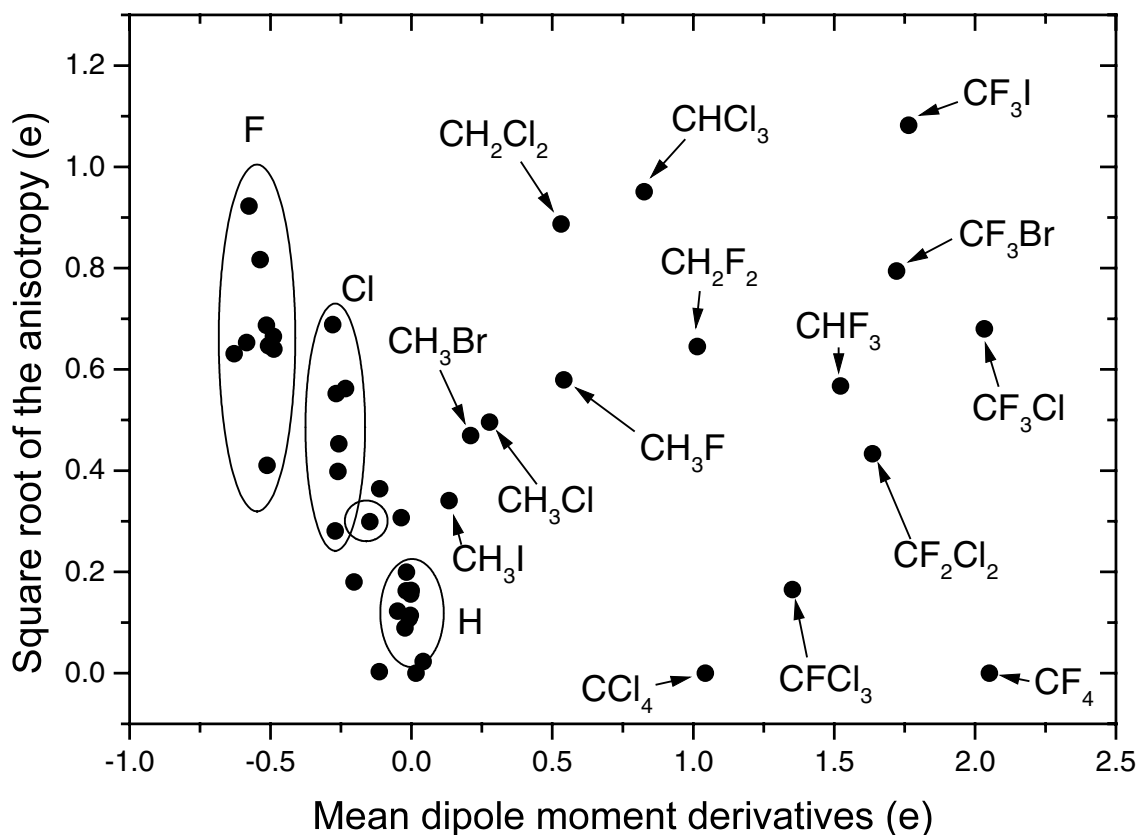
Fig. 1. Graph of the square root of the atomic anisotropy, β_α, versus the atomic mean dipole moment derivative, $\bar{p}_\alpha$. Fluorine, chlorine and hydrogen atom groups are identified as well as the molecules of some of the carbon atom points.

The square of the atomic effective charge, χ_α^2, is 1/3 the trace of the matrix product of the atomic polar tensor by its transpose

$$\chi_\alpha^2 = 1/3 \, \mathrm{Tr}(\mathbf{P}_x^{(\alpha)}\mathbf{P}_x^{(\alpha)'}). \tag{6}$$

This is simply equal to 1/3 the sum of squares of the APT elements. The atomic anisotropy,

$$\beta_\alpha^2 = (1/2)[(p_{xx} - p_{yy})^2 + (p_{yy} - p_{zz})^2 + (p_{zz} - p_{xx})^2$$

$$+ 3(p_{xy}^2 + p_{yz}^2 + p_{xz}^2 + p_{zx}^2 + p_{yx}^2 + p_{zy}^2)] \tag{7}$$

is another invariant and is related to $\bar{p}_\alpha^2$ and χ_α^2 by the following equation

$$\chi_\alpha^2 = \bar{p}_\alpha^2 + \left(\frac{2}{9}\right)\beta_\alpha^2. \tag{8}$$

The determinant and the sum of minors are calculated by the usual equations.

The polar tensor invariant values for methane [10], the fluoromethanes [9,11–17], chloromethanes [18–23], fluorochloromethanes [24], CH$_3$Br [18,25], CH$_3$I [18], CF$_3$Br [26] and CF$_3$I [26] are given in Table 1. These values were subjected to a principal component analysis [27,28]. The data matrix, $\mathbf{X}$, was 45×5, each row containing an atomic polar tensor set of invariant quantities and each column corresponding to one of the invariant quantities. The principal components are the eigenvectors of the $\mathbf{X}'\mathbf{X}$ matrix product and are linear combinations of the APT invariant quantities. The principal component space is related to the APT invariant space by rotations that maximize the data variances on the first principal components. For this reason principal component transformations can be used to reduce the dimensionality of a data analysis problem without
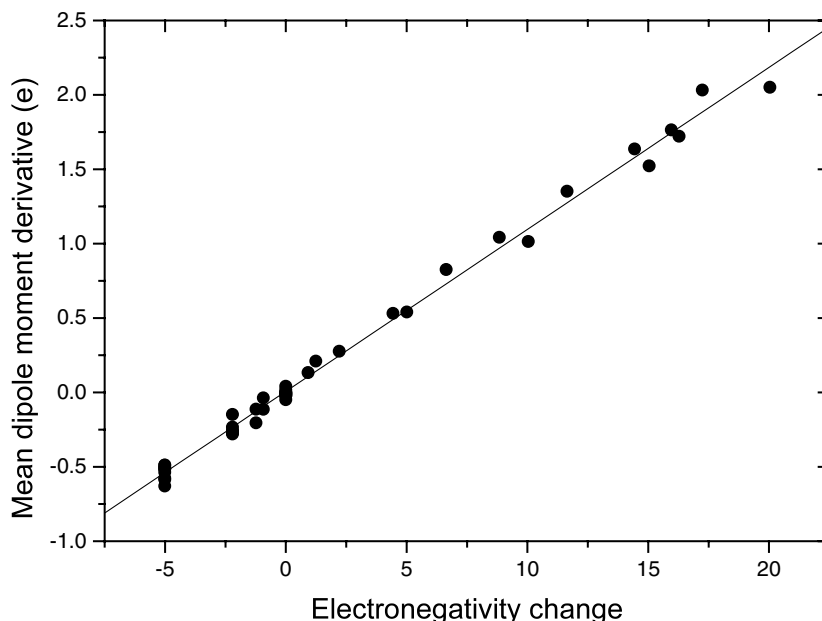
Fig. 2. The graph of the mean dipole moment derivative, $\bar{p}_\alpha$, versus the substituent electronegativity change defined in the text.

losing significant statistical information. In other words the principal component transformation permits an exploratory multidimensional data analysis that provides information on which graphs involving the untransformed variables are the most useful to examine in modeling attempts. These graphs are presented and discussed in the remainder of this paper.

3. Results

Three principal components explain 99% of the total data variance and indicate that the most informative graph involving the original variables is the one obtained by plotting any of the four invariants, $\bar{p}_\alpha$, χ_α, $D_\alpha^{1/3}$, $C_\alpha^{1/2}$, against β_α. Since $\bar{p}_\alpha$ is conceptually the simplest invariant to understand among the four, its graph against β_α is shown in Fig. 1. Two main trends are evident in the graph. One of them is seen for the terminal atom derivatives that form separate groups for H, Cl and F atoms and are correlated with their own electronegativities. All the fluorine atom's $\bar{p}$ values are around $-0.5e$, the chlorine ones around $-0.25e$ and all hydrogen ones are almost zero. As the substituent electronegativity increases the value of $\bar{p}_X$ (X = H, I, Br, Cl and F) becomes more negative.

The terminal atom's $\bar{p}_X$ values show a much smaller variation -0.5 to $0e$, than the one found for the carbon atoms, $0-2e$, for which the other trend is evident. As the sum of the substituent atom electronegativities increases the corresponding $\bar{p}_C$ values increase proportionally. For this reason it seems fruitful to investigate the behavior of $\bar{p}_C$ as a function of substituent electronegativity sum.

In Fig. 2 $\bar{p}_\alpha$ is graphed as a function of electronegativity change upon halogen substitution in methane, ΔE, calculated using the Mulliken–Jaffe scale [29]. The electronegativity change in the carbon atom of a halomethane relative to the one in methane is given by a sum of the electronegativities of the substituent atoms minus this sum in methane. The electronegativity change in a substituent is taken as the difference between the hydrogen atom and substituent atom electronegativity. This way negative changes are obtained for the substituents, consistent with their expected negative charges. Positive changes, on the other hand, are obtained for the carbon atoms that are expected to be positively charged in the halomethanes. The plot in Fig. 2 shows a very clear linear dependence of $\bar{p}_\alpha$ on electronegativity change and has a correlation coefficient of 0.997. This evidence points to an interpretation of $\bar{p}_\alpha$ as an atomic charge. This is consistent

Table 2
Experimental fundamental intensity sums and those calculated using Eq. (11). Units of km mol^{-1}

Molecule	$\sum A_i$ (Eq. (11))	$\sum A_i$ (Experimental)	$K^{-1}\Omega$ [53]	$\sum A_i$ [3]
CH_4	95.5	97.3 [35], 100.0 [36], 107.6 [37], 104.0 [38]	0.0	77.5
CH_3F	178.3	192.9 [39], 194.2 [40]	14.6	194.0
CH_2F_2	420.2	393.7 [41], 442.0 [42], 409.4 [14]	6.4	449.6
CHF_3	789.9	784.3 [15], 751.4 [43], 749.0 [44]	6.6	813.4
CF_4	1302.7	1341.5 [38], 1219.8 [45] 1208.6 [46]	0.0	1299.2
CH_3Cl	89.1	77.3 [19], 73.6 [47], 73.7 [39], 73.7 [40], 75.2 [48]	8.7	85.2
CH_2Cl_2	117.7	138.9 [49], 173.6 [42]	7.8	125.5
$CHCl_3$	180.1	262.7 [50], 253.3 [21]	0.6	194.5
CCl_4	261.5	322.2 [50]	0.0	278.3
CF_3Cl	978.3	972.4 [51], 1271.9 [52]	0.1	987.9
CF_2Cl_2	696.8	819.8 [42]	0.1	715.1
$CFCl_3$	457.8	550.5 [53]	0.1	478.5
CH_3Br	78.2	62.3 [47], 63.9 [40]	3.8	69.3
CH_3I	76.2	56.1 [47], 55.3 [40]	2.4	66.0
CF_3Br	885.2	959.9 [54]	0.0	901.1
CF_3I	855.5	1063.8 [53]	0.0	873.5

with the fact that $\bar{p}_C$ has been shown to be an adequate estimate of carbon atomic charges for estimating ionization energies of 1s electrons on the carbon atom using Siegbahn's simple potential model [30].

4. Discussion

An important objective of this research on infrared vibrational intensities is their estimation by empirical or theoretical models since their accurate experimental measurement is difficult. Transference of electro-optical parameters [31] or atomic polar tensors [32] results in intensity estimates that are capable of resolving problems in applications where symmetry-based selection rules are not sufficiently accurate. Quantum chemical intensity estimates have been useful in other applications, such as resolving sign ambiguities [33] of dipole moment derivatives. In this report we present an empirical model that permits the calculation of intensity sums for the halomethanes using only atomic masses and the electronegativities of substituent atoms. This will hopefully increase the under-standing of infrared intensity sum results in terms of simple chemical concepts.

The G intensity sum rule proposed by Crawford [34],

$$\sum A_i + \Omega = K \sum \left(\frac{\chi_\alpha^2}{m_\alpha} \right), \tag{9}$$

relates the fundamental intensity sum, $\sum A_i$, plus a usually small rotational correction, Ω, to a sum of squared atomic effective charges, χ_α^2, divided by their corresponding atomic masses, m_α for all atoms in the molecule. Since $\bar{p}_\alpha$ results in an excellent fit with the electronegativity changes defined previously and $\bar{p}_\alpha$ and χ_α absolute values are highly correlated (>0.99), χ_α also results in an excellent linear fit with the electronegativity changes where

$$\chi_\alpha = 0.08975 + 0.10554(\Delta E) \tag{10}$$

with ΔE representing the electronegativity changes defined earlier. Substitution of this expression in the G sum rule and use of the 2924.7 constant for K corresponding to units of km mol^{-1} for A, e for χ_α
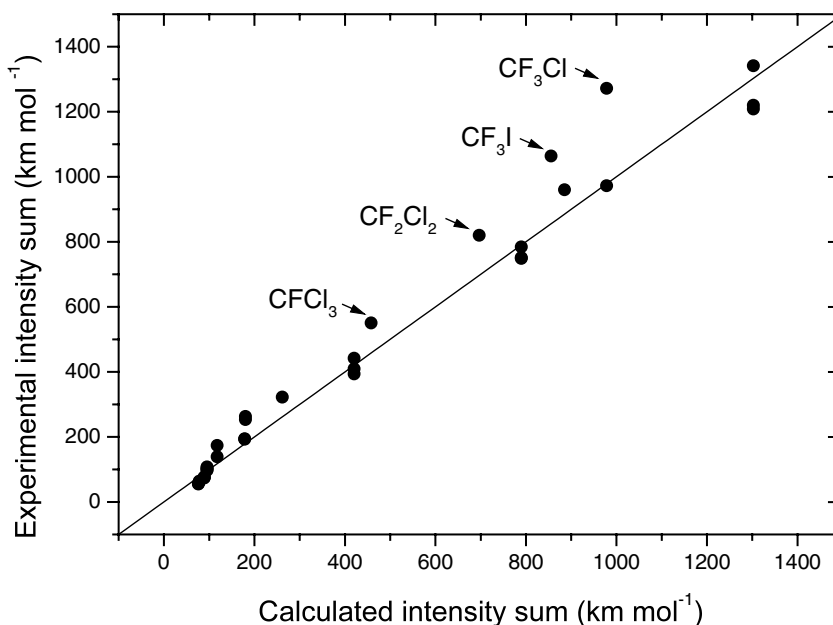
Fig. 3. Graph of the experimental intensity sums plotted against the sums predicted by the proposed model. The line represents exact agreement.

and amu for m_α results in the following equation,

$$\sum A_i + \Omega = 23.56\left[\left(\frac{1}{m_C}\right) + \left(\sum_X \frac{1}{m_X}\right)\right]$$

$$+55.41\left\{\left[\frac{\left(\sum_X E_X\right)}{m_C}\right] - \left[\sum_X \left(\frac{E_X}{m_X}\right)\right]\right\}$$

$$+32.58\left\{\left[\frac{\left(\sum_X E_X\right)^2}{m_C}\right] + \left[\sum_X \left(\frac{E_X^2}{m_X}\right)\right]\right\}, \quad (11)$$

where the X index represents the substituent atoms in the halomethanes. The Mulliken–Jaffe electronegativity values of H, F, Cl, Br and I are 7.17, 12.18, 9.38, 8.40 and 8.10, respectively. For use in the above equation, electronegativity values relative to a zero value for hydrogen are to be used, i.e. 0.00 (H), 5.01 (F), 2.21 (Cl), 1.23 (Br) and 0.93 (I).

The results for $\sum A_i$ obtained from this empirical model and the corresponding experimental values [14,15,19,21,35–54] are given in Table 2. The rota-

tional corrections, Ω, for the fluoromethanes, chloromethanes and fluorochloromethanes were taken from Ref. [53] and have been included in Table 2.

For most of the molecules the experimental intensity sums were taken from several sources. In most cases the sum values agree within about 10% of their average values. Only for the CF$_3$Cl data is the precision much worse, with the deviation between the literature values being about 25% of their average value. Review of Fig. 3 clearly shows this discrepancy in the experimental intensity sums of CF$_3$Cl. For most of the molecules in Table 2 the agreements between the empirical model prediction and the experiment are very good except for CFCl$_3$, CF$_2$Cl$_2$, CF$_3$I and for one of the CF$_3$Cl experimental results. Note that the experimental value for CF$_3$Cl in agreement with the model prediction was measured twenty years later than the result showing large deviation. However, the model, given by Eq. (11), might under-estimate some halomethane intensity sums. Only one experimental intensity sum has been listed in Table 2 for CF$_2$Cl$_2$ [42] and CFCl$_3$ [53] since, to our knowledge, only one research group has measured all the fundamental gas phase intensities for each of these molecules. However, the values in Table 2 for the intensity sums of these molecules have been

confirmed by independent measurements later. For example, $CFCl_3$ has only two strong bands contributing 549 km mol^{-1} to the total intensity sum of 550.5 km mol^{-1}, i.e. 99.7% of the intensity sum. Since the strong bands occur in the atmospheric window and interest in measuring Freon concentrations in the atmosphere is high, these two bands have been reinvestigated by several research groups. The intensity sum for the two strong bands was found to be 576 [55], 534 [56] and 526 km mol^{-1} [57], in good agreement with the values reported by Person et al. [53]. The CF_2Cl_2 molecule has three strong bands that contribute 98% of the total intensity reported in Ref. [42], i.e. 804 km mol^{-1}. This value is also in very good agreement with values determined later, 773 [55] and 800 km mol^{-1} [58] for the intensity sum of these three bands.

The empirical model proposed here predicts most of the trends in the intensity sums owing to substituent changes in methane. As fluorine atoms are substituted for hydrogen in methane the experimental intensity sum increases by about 100 km mol^{-1} for the first substitution, by another 200 km mol^{-1} for the second one, 350 km mol^{-1} for the third and almost 500 km mol^{-1} for the last substitution. The empirical model predicts this nonlinear behavior quite well with corresponding increases of 80, 240, 370 and 510 km mol^{-1}. For chlorine substitution in methane the model is capable of qualitatively reproducing the intensity sum trend on substitution. Just as for the experimental intensities, the sum for methane is predicted to be larger than the one for methyl chloride whereas a further chlorine substitution results in increasingly larger intensity sums for CH_2Cl_2, $CHCl_3$ and CCl_4. However, the model underestimates the magnitude of these changes. The model correctly predicts increasing intensity sums when fluorine is substituted for chlorine in the fluorochlormethanes. The experimental intensity sums decrease in the order CH_3F, CH_3Cl, CH_3Br and CH_3I as the electronegativity of the substituted halogen decreases. As expected the empirical model predicts the same trend. Again the intensity sum of the methane molecule does not follow this simple pattern since its sum is less than the one for CH_3F though more than the one for CH_3Cl. The empirical model correctly predicts this ordering. Besides the electronegativity effect the change in atomic mass is also important, especially for the hydrogen atom since its reciprocal mass provides a positive contribution in the first term of Eq. (11) and is much larger than the reciprocal masses of the other atoms in these molecules. Although the model is not successful in accurately predicting the experimental values for the halomethanes studied here it does correctly predict the general trend in values. As the X = F, Cl, Br, I and H substituent changes in the CF_3X molecules the model predicts intensity sum decreases. This agrees with the trend observed in the averages of the experimental intensity sums except for the ordering of these values for CF_3Br and CF_3I.

The last column of Table 2 contains intensity values estimated by the empirical intensity model proposed in Ref. [1]. The model proposed there uses two linear regressions, one for the carbon atoms and another for the terminal atoms. The results from both models are in excellent agreement as expected. Besides having the advantage of using only one regression equation, the intensity sum can be calculated directly using Eq. (11) and shows the importance of both the electronegativity and atomic mass effects very clearly.

Acknowledgements

References

[1] B.B. Neto, M.M.C. Ferreira, I.S. Scarminio, R.E. Bruns, J. Phys. Chem. 93 (1989) 1728.
[2] B.B. Neto, I.S. Scarminio, R.E. Bruns, J. Chem. Phys. 89 (1988) 89.
[3] B.B. Neto, R.E. Bruns, J. Phys. Chem. 94 (1990) 1764.
[4] P.H. Guadagnini, A.E. de Oliveira, R.E. Bruns, B.B. Neto, J. Am. Chem. Soc. 119 (1997) 4224.
[5] J. Overend, in: M. Davies (Ed.), Infrared Spectroscopy and Molecular Structure, Elsevier, Amsterdam, 1963 (chap. 10).
[6] W.B. Person, J.H. Newton, J. Chem. Phys. 61 (1974) 1040.
[7] J.F. Biarge, J. Herranz, J. Morcillo, Ann. R. Soc. Esp. Fis. Quim. A 57 (1961) 81.
[8] E.B. Wilson, J.C. Decius, P.C. Cross, Molecular Vibrations, McGraw-Hill, New York, 1955.
[9] J.H. Newton, W.B. Person, J. Chem. Phys. 64 (1976) 3036.
[10] A.E. de Oliveira, P.H. Guadagnini, R. Custódio, R.E. Bruns, J. Phys. Chem. 102 (1998) 4615.

[11] E. Suto, H.P. Martins F, R.E. Bruns, J. Mol. Struct. (Theochem) 282 (1993) 81.

[12] S. Kondo, S. Saeki, J. Chem. Phys. 76 (1982) 809.

[13] E. Suto, R.E. Bruns, B.B. Neto, J. Phys. Chem. 95 (1991) 9716.

[14] S. Kondo, T. Nakanaga, S. Saeki, J. Chem. Phys. 73 (1980) 5409.

[15] S. Kondo, S. Saeki, J. Chem. Phys. 74 (1981) 6603.

[16] K. Kim, W.T. King, J. Chem. Phys. 73 (1980) 5591.

[17] A.E. de Oliveira, R.L.A. Haiduke, R.E. Bruns, Spectrochim. Acta A 56 (2000) 1329.

[18] H.P. Martins F, R.E. Bruns, J. Phys. Chem. 97 (1993) 4345.

[19] S. Kondo, Y. Koga, T. Nakanaga, S. Saeki, Bull. Chem. Soc. Jpn 56 (1983) 416.

[20] H.P. Martins F, J.B.L. de Oliveira, R.E. Bruns, J. Mol. Struct. (Theochem) 335 (1995) 113.

[21] K. Kim, W.T. King, J. Chem. Phys. 80 (1984) 978.

[22] E. Suto, M.M.C. Ferreira, R.E. Bruns, J. Comput. Chem. 12 (1991) 885.

[23] A.E. de Oliveira, R.E. Bruns, Spectrochim. Acta A 55 (2000) 2215.

[24] H.P. Martins F, J.B.L. de Oliveira, P.H. Guadagnini, R.E. Bruns, J. Phys. Chem. 99 (1995) 11 357.

[25] A.J. van Straten, W.M.A. Smit, J. Chem. Phys. 67 (1977) 970.

[26] H.P. Martins F, P.H. Guadagnini, J. Mol. Struct (Theochem) 464 (1999) 171.

[27] K.U. Mardia, J.T. Kent, J.M. Bibby, Multivariate Analysis., Academic Press, London, 1979 (chap. 8).

[28] B.B. Neto, M.M.C. Ferreira, I.S. Scarminio, R.E. Bruns, J. Phys. Chem. 93 (1989) 1728.

[29] J.E. Huheey, J. Phys. Chem. 69 (1965) 3284.

[30] K. Siegbahn, C. Nordling, G. Johansson, J. Hedman, P.F. Heden, K. Hamrin, U. Gelius, T. Bergmark, L.O. Werme, R. Manne, Y. Baer, ESCA Applied to Free Molecules, North-Holland, Amsterdam, 1969.

[31] G. Zerbi, in: W.B. Person, G. Zerbi (Eds.), Vibrational Intensities in Infrared and Raman Spectroscopy, Elsevier, Amsterdam, 1982 (chap. 3).

[32] W.B. Person, in: W.B. Person, G. Zerbi (Eds.), Vibrational Intensities in Infrared and Raman Spectroscopy, Elsevier, Amsterdam, 1982 (chap. 14).

[33] R.E. Bruns, in: W.B. Person, G. Zerbi (Eds.), Vibrational Intensities in Infrared and Raman Spectroscopy, Elsevier, Amsterdam, 1982 (chap. 7).

[34] B.L. Crawford Jr., J. Chem. Phys. 20 (1952) 977.

[35] J.H.G. Bode, W.M.A. Smit, J. Phys. Chem. 84 (1980) 198.

[36] K.J. Kim, J. Quant. Spectrosc. Radiat. Transfer 37 (1987) 107.

[37] J. Heicklen, Spectrochim. Acta A 17 (1961) 201.

[38] S. Saeki, S. Mizuno, S. Kondo, Spectrochim. Acta A 32 (1976) 403.

[39] J.W. Russell, C.D. Needham, J. Overend, J. Chem. Phys. 45 (1966) 3383.

[40] G.M. Barrow, D.C. McKean, Proc. R. Soc. London Ser. A 213 (1952) 27.

[41] M. Mizuno, S. Saeki, Spectrochim. Acta A 32 (1976) 1077.

[42] J. Morcillo, L.R. Zamarano, J.M.V. Heredia, Spectrochim. Acta A 22 (1966) 1969.

[43] R.W. Levine, W.B. Person, J. Phys. Chem. 81 (1977) 1118.

[44] S. Sofue, K. Kawoguchi, E. Hirota, T. Fujiyama, Bull. Chem. Soc. Jpn 54 (1981) 3546.

[45] C.M. Roehl, D. Boglu, C. Bruhl, G.K. Moortgat, Geophys. Res. Lett. 22 (1995) 815.

[46] B. Schurin, J. Chem. Phys. 30 (1959) 1.

[47] A.D. Dickson, I.M. Mills, B.L. Crawford Jr., J. Chem. Phys. 27 (1957) 445.

[48] J.W. Elkins, R.H. Kagan, R.L. Sams, J. Mol. Spectrosc. 105 (1984) 480.

[49] S. Saeki, K. Tanabe, Spectrochim. Acta A 25 (1969) 1325.

[50] K. Tanabe, S. Saeki, Spectrochim. Acta A 26 (1970) 1469.

[51] W.G. Golden, D. Horner, J. Overend, J. Chem. Phys. 68 (1978) 964.

[52] J. Herranz, R. de la Cierva, J. Morcillo, An. Real Soc. Espan. Fis. Quim. (Madrid) A 55 (1959) 69 (as reported in Ref. [50]).

[53] W.B. Person, S.K. Rudys, J.H. Newton, J. Phys. Chem. 79 (1975) 2525.

[54] W.B. Person, S.R. Polo, Spectrochim. Acta A 17 (1961) 101.

[55] P. Varanasi, F.K. Ko, J. Quant. Spectrosc. Radiat. Transfer 17 (1977) 385.

[56] Z. Li, P. Varanesi, J. Quant. Spectrosc. Radiat. Transfer 52 (1994) 137.

[57] R. Names, P.M. Silvaggio, R.W. Boese, J. Quant. Spectrosc. Radiat Transfer 23 (1980) 211.

[58] P. Varanasi, S. Chudamani, J. Quant. Spectrosc. Radiat. Transfer 39 (1988) 193.